Title

Stem respiration and growth in a central Amazon rainforest

Journal

Trees, 36(3)

ISSN

0931-1890

Authors

Jardine, Kolby J
Cobello, Leticia O
Teixeira, Liliane M
et al.

Publication Date

2022-06-01

DOI

10.1007/s00468-022-02265-5

Peer reviewed

Stem respiration and growth in a central Amazon rainforest

Kolby J. Jardine[1,2]*, Leticia O. Cobello[2], Liliane M. Teixeira[2], Malyia-Mason S. East[1], Sienna Levine[1], Bruno O. Gimenez[2,4], Emily Robles[1], Gustavo Spanner[2], Charlie Koven[1], Chongang Xu[3], Jeffrey M. Warren[5], Niro Higuchi[2], Nate McDowell[6,7], Gilberto Pastorello[1], Jeffrey Q. Chambers[1,2,8]

[1]Lawrence Berkeley National Laboratory, Climate and Ecosystem Sciences Division, Berkeley, CA, USA

[2]National Institute for Amazon Research, Manaus, Amazonas, Brazil

[3]Los Alamos National Laboratory, Earth and Environmental Sciences Division, Los Alamos, NM, USA

[4]Smithsonian Tropical Research Institute, Panama City, Panama

[5]Oak Ridge National Laboratory, Environmental Sciences Division, Oak Ridge, TN, USA

[6]Pacific Northwest National Laboratory, Atmospheric Sciences and Global Change Division, Richland, WA, USA

[7]Washington State University, School of Biological Sciences, Pullman, WA, USA

[8]University of California Berkeley, Department of Geography, Berkeley, CA, USA

*corresponding author: kjjardine@lbl.gov

Abstract

Tropical forests cycle a large amount of CO_2 between the land and atmosphere, with a substantial portion of the return flux due tree respiratory processes. However, *in situ* estimates of woody tissue respiratory fluxes and carbon use efficiencies (CUE_W) and their dependencies on physiological processes including stem wood production (P_w) and transpiration in tropical forests remain scarce. Here, we synthesize monthly P_w and daytime stem CO_2 efflux (E_S) measurements over one year from 80 trees with variable biomass accumulation rates in the central Amazon. On average, carbon flux to woody tissues, expressed in the same stem area normalized units as E_S, averaged 0.90 ± 1.2 μmol m^{-2} s^{-1} for P_w, and 0.55 ± 0.33 μmol m^{-2} s^{-1} for daytime E_S. A positive linear correlation was found between stem growth rates and stem CO_2 efflux, with respiratory carbon loss equivalent to 15 ± 3% of stem carbon accrual. CUE_W of stems was non-linearly correlated with growth and was as high as 77-87% for a fast-growing tree. Diurnal measurements of stem CO_2 efflux for three individuals showed a daytime reduction of E_S by 15-50% during periods of high sap flow and transpiration. The results demonstrate that high daytime E_S fluxes are associated with high CUE_W during fast tree growth, reaching higher values than previously observed in the Amazon Basin (e.g. maximum CUE_W up to 77-87%, versus 30-56%). The observations are consistent with the emerging view that diurnal dynamics of stem water status influences growth processes and associated respiratory metabolism.

Keywords: tropical trees, ecophysiology, NPP, GPP, NEE, NEP, CO_2, stem respiration, tree growth, forest disturbance

Statements and Declarations: The authors have no conflicts of interest to declare that are relevant to the content of this article.

Key Message: Annual stem CO_2 efflux increases with stem wood production rates and are inhibited by daily moisture stress

1. Introduction

The Amazonian forest fixes more atmospheric CO_2 than any other terrestrial ecosystem (Nobre et al. 2016). However, observations have suggested that the majority of tree assimilated carbon (~70% in the Central Amazon) is returned to the atmosphere through autotrophic respiration, resulting in low carbon use efficiency (CUE) (Amthor 2000a; Valentini et al. 2000; Chambers and Silver 2004; Rowland et al. 2014). Biologically, autotrophic respiration provides chemical energy, reducing power, and carbon skeletons needed in innumerable physiological processes including growth and development, tissue maintenance including biosynthesis of defensive and signaling compounds during abiotic and biotic stress responses, and reproduction and senescence processes (O'Leary et al. 2019). Mitochondrial respiratory activity is also critical for optimizing photosynthetic metabolism, including during periods of stress which can lead to over-reduction of mitochondria and/or chloroplasts and excessive production of reactive oxygen species (Vanlerberghe et al. 2020). Given that field observations and modeling activities have primarily focused on photosynthesis as a primary control over net primary productivity (NPP), our predictive understanding of autotrophic respiration and its dependencies on biological and environmental factors is less advanced than that of photosynthesis (Amthor 2000b; Atkin and Macherel 2009). Thus, our predictive understanding of tropical forest-atmosphere carbon exchange is incomplete, particularly with respect to tree carbon allocation into both anabolic (biosynthesis of biopolymers and metabolites used in new biomass production such as structural and non-structural carbohydrates and defense compounds) and catabolic (e.g. respiration of stored and recently assimilated substrates) pathways (Chambers and Silver 2004; Clark 2004; Feeley et al. 2007; Lloyd and Farquhar 2008; Körner 2009). However, quantifying sensitivities of key anabolic and catabolic metabolism responses to abiotic and biotic stress conditions as mediated by plant physiological processes (e.g., photosynthesis, transpiration, and growth) in diverse tropical forests, remains a grand challenge.

The importance of autotrophic respiration in the global carbon cycle is highlighted by estimates of global terrestrial autotrophic respiration of 45–55 Pg C/yr of CO_2 (Luyssaert et al. 2007), which is 4.5-6.2 times the average annual CO_2 release from anthropogenic fossil fuel combustion over 2008-2017 (8.9-9.9 Pg C/yr of CO_2) (Le Quéré et al. 2018). Although highly uncertain in the tropics, autotrophic respiration can be more than 50% of total ecosystem respiration in tropical wet forests. In the central Amazon near the city of Manaus, Brazil for example, total autotrophic respiration was an estimated 68% of total ecosystem respiration (Malhi et al. 2009).

Respired CO_2 within tree stems can diffuse to the atmosphere driven by the concentration gradient between the inner bark and ambient air (McGuire and Teskey 2004; Aubrey and Teskey 2009). This mechanism is known as stem CO_2 efflux (E_S, μmol m^{-2} s^{-1}) and is estimated to represent a large but uncertain fraction of autotrophic respiration in tropical forest ecosystems (Chambers et al. 2004; Trumbore 2006; Malhi et al. 2009). E_S is an important regulator of the internal fluxes of CO_2 in plants and has been mathematically described by **Eq. 1**, where R_{stem} is stem respiration, E_S is net stem CO_2 efflux (μmol m^{-2} s^{-1}), F_T is net CO_2 transport flux vertically through the xylem (μmol m^{-2} s^{-1}), and ΔS is change in CO_2 storage concentration (ppm s^{-1}) (McGuire and Teskey 2004).

Equation 1: $R_{stem} = E_S + F_T + \Delta_S$

Although limited observations have been reported in the Amazon Basin, stem respiration can represent a major fraction (21.2%) of total autotrophic respiration (Malhi et al. 2009), with mean annual E_S fluxes of 0.6 μmol m^{-2} s^{-1} reported for trees in the central Amazon (Chambers et al. 2004; Trumbore 2006) and the Tapajos National Forest (Nepstad 2002). Slightly higher mean annual Es fluxes of 1.0 ± 0.1 μmol m^{-2} s^{-1} were reported from the Caxiuanã National Forest reserve in the eastern Amazonia (Rowland et al. 2018). Outside of the Basin, studies in other Neotropical forest sites have reported fluxes between 1.0-1.5 μmol m^{-2} s^{-1} in French Guiana with a large seasonal variation during climatic transition periods (Stahl et al. 2011) and 0.83-1.24 μmol m^{-2} s^{-1} for two canopy trees in a Costa Rica forest where E_S was highly positively correlated with annual wood production rates (P_w) (Ryan et al.

1994). Although not yet reported in a tropical forest, on a diurnal time scale, a growing number of greenhouse and mid-latitude field studies have shown a suppression of E_S efflux during the day associated with high transpiration rates (Levy et al. 1999; Wittmann et al. 2006; Maier and Clinton 2006; Saveyn et al. 2007; Teskey and McGuire 2007; Bowman et al. 2008).

Characterizing the dependencies of E_S on biological and environmental variables in diverse tropical forests is central to reducing the high uncertainties surrounding the quantitative importance of stem respiration in the tropics. We hypothesize that a direct linkage between carbon allocation to the stem and R_{stem} exists such that high stem growth results in an increased demand for both carbon skeletons used in new biomass construction as well as respiratory substrates for energy production to meet the increased biosynthetic demands. Thus, we hypothesize that stem growth is positively correlated stem respiration. This is because a higher stem growth rates will require an increased demand for both carbon skeletons used in new biomass construction as well as respiratory substrates for energy production to meet the increased biosynthetic demands. This hypothesis predicts that if R_{stem} increases due to increased energy demands associated with rapid cell division and biopolymer biosynthesis, based on Eq. 1 and assuming no change to F_t and ΔS, E_S should correspondingly increase. We also hypothesize that there is a suppression of daytime respiration during the noon, despite high rates of canopy photosynthesis in combination with the higher daytime temperatures. This is because daytime xylem tension could potentially suppress the demand for respiratory substrates in the sapwood. We test these hypotheses by analyzing monthly observations of basal stem E_S and stem diameter for 80 trees in stands with variable biomass accumulation rates within permanent plots of a long-term forest dynamics experiment (known as BIONTE) in central Amazon forests (Higuchi et al. 1997). We also characterized diurnal patterns of basal E_S in three canopy trees at the nearby K34 tower together with diurnal observations of physiological and environmental drivers. Diurnal observations were made of crown temperature (27 m – 31 m), vapor pressure deficit (VPD) between the upper canopy and the atmosphere

126 (28 m), as well as sap velocity and stem E_S fluxes at the base of the trees (1.7-2.1 m).

127

128 **2. Materials and Methods**

129 *2.1 Monthly observations of stem growth and CO_2 efflux in the BIONTE experiment*

130 The field experiment was carried out at the Experimental Station of Tropical Forestry (EEST/
131 ZF-2) 60 km northwest of Manaus/Brazil, which has 23,000 ha of undisturbed forest. We first
132 characterized potential dependencies of E_S on stem growth rates in forests north of Manaus, Brazil,
133 using data from a selective logging experiment (BIONTE). BIONTE (the BIOmass and NuTrient
134 Experiment) (S2º 38' 17", W60º 09' 25") is a long-running study of forest response to experimental
135 logging carried out in forests north of Manaus along the ZF-2 road, and managed by scientists at
136 Brazil's National Institute for Amazon Research (Instituto Nacional de Pesquisa da Amazônia –
137 INPA) (Otani et al. 2018). The experiment consists of three blocks of 24 ha forest, with treatment
138 replicated in each block, for a total of three replicates per treatment. Selective logging treatments were
139 conducted in the mid-1980s and comprised three levels of commercial tree removal (not total) based
140 on species-specific basal area (T1 =32%, T2 = 42%, T3 = 69%), and control plots with no logging
141 (T0). A total of 12 ha (9 treatment, 3 control) were established in the central-most area of each 4-ha
142 replicate (**Fig. 1**). Tree recruitment, growth and mortality were measured annually following logging
143 in all plots, with the exception of two missing years (1994 and 1998). Tree growth was determined by
144 the mean annual change in tree base diameter (measured at 1.3 m height, or above the buttresses).
145 Wood density was used to estimate mean annual wood production rates, or P_w, for all trees in each
146 replicate plot (12 ha total).

147 A stem respiration study was carried out to explore changes in stem CO_2 efflux (E_S) as a
148 function of plot-level biomass accumulation rates, and with variation in tree growth rates and stem
149 diameter, in 2002. Four trees were randomly selected from five tree growth rate classes for each
150 treatment block, for a total of 20 trees per treatment block, or 80 trees total from the BIONTE plots with

stem diameters ranging from 10 to 52 cm. All species were previously identified by comparing botanical vouchers to an herbarium reference collection organized by the Biological Dynamics of Forest Fragments Project (BDFFP) at the National Institute for Amazon Research (INPA) and also by consulting specialists for taxonomic verification (Gaui et al., 2019). Botanical identification followed the "Angiosperm Phylogeny Group – APG" (APG III, 2009) classification system. Each of the 80 trees selected for the E_S study were outfitted with dendrometer bands (da Silva et al. 2002) to increase the precision and accuracy of diameter growth rate measurements. The dendrometer bands were placed on the trees at least 6 months before initiating monthly measurements from January 2002-November 2002 (note, stem diameter measurements were not made during October 2002). The dendrometers were measured with digital calipers on the same days as the respiration measurements. Stem E_S was measured using the static enclosure method described previously (Chambers et al. 2004). Briefly, an infra-red gas analyzer (LiCor 820) was operated as a closed dynamic chamber with a flow rate of 1.0 L min^{-1}. Polyvinyl chloride (PVC) semi-cylindrical chambers (250–400 mL) were cinched to the tree stem just above the dendrometer bands at 1.3 m height using nylon straps, creating a reasonably air-tight seal. The measurement interval spanned 1–2 min, and the E_S from the stem of each tree was quantified from the slope of the increase in $[CO_2]$ versus time in the static enclosure and the area of the enclosed stem (μmol CO_2 m^{-2} s^{-1}). Stem E_S for each of the 80 trees in the BIONTE plots was determined during May, June, July, August, and September of 2002. At the end of the monthly E_S measurement period, a small wooden plug was removed from the base of each tree using a tenon cutter (extracting a dowel of wood) and power drill. The wood plug was used to determine wood density D (g dry weight/mL wet volume), enabling calculation of stem growth rates in the same units as stem respiration (μmol CO_2 m^{-2} s^{-1}). Together with unit conversion, the average annual stem growth rate expressed as CO_2 capture (Stem_growth_CO_2) was calculated according to **Eq. 2** where DBH_increment is the average annual diameter increment (μm day^{-1}). By plotting the average annual E_S flux versus the average annual stem growth rate expressed as a CO_2 flux in μmol CO_2 m^{-2} s^{-1} for each of the 80 individuals in the

BIONTE plots during 2002, the slope of the regression line represents the net respiratory carbon loss to the atmosphere normalized to stem carbon accrual, while the intercept equals the maintenance respiration (R_M) (McDowell et al., 1999). Finally, the average annual carbon use efficiency of woody tissue (CUEw) for each individual was estimated using **Eq. 3**. CUEw was estimated for each individual using both the observed average daytime E_S fluxes, as well as nighttime E_S fluxes which were assumed to be 2-times higher during the night than during the day based on results from the diurnal E_S studies described in section 2.2.

Equation 2: Stem_growth_CO_2 (μmol CO_2 m^{-2} s^{-1}) = DBH_increment (μm day^{-1}) x 1.157E-5 (day/s) x D (g/ml) x 10^{-12} ml/μm^3 x 10^{12} $\mu m^2/m^2$ x 1 mol CO_2/44 g x 10^6 μmol/mol CO_2

Equation 3: CUEw = Stem_growth_CO_2/(Stem_growth_CO_2 + Es) x 100%

2.2 Continuous observations of crown temperature, sap velocity, and E_s during the night and day for three trees near the K-34 tower

While the observations in the BIONTE experiment focused on average annual relationships between stem growth and Es fluxes during the day, a second study was carried out at the nearby K34 tower within the ZF2 forest preserve to evaluate potential diurnal patterns in E_S, and potential correlations with temperature and transpiration. These observations took advantage of both continuous line power for real-time sensors (sap velocity, high precision dual channel CO_2 gas analyzer, as well as the tower structure for collecting crown temperature and VPD from above canopy sensors mounted on the tower). In contrast to the BIONTE study (and other previous studies in the tropics) where the buildup of CO_2 within a static stem enclosure was used to estimate E_S 'snapshots' during the day, the K34 tower experiment utilized a dynamic stem enclosure where ambient air continuously entered the

stem chamber with CO_2 efflux estimated from the CO_2 concentration difference between ambient air entering the enclosure and air exiting the stem chamber.

Due to logistical issues of working at the remote tropical rainforest site during rainy conditions (site access challenges, power failures, liquid water inside stem chamber and tubing, etc.), only 1 day and 1 day-night transition E_S data set was collected for each tree individual. Trees were selected based on the crown proximity to the remote K34 tower, which enabled sap velocity, canopy temperature, and vapor pressure deficit (VPD) measurements by providing line power for the sensors and a mounting structure for sensors as a part of the Large-Scale Biosphere-Atmosphere Program (LBA). Three canopy trees including *Pouteria anomala* (Pires) T.D.Penn (35.3 cm of DBH, 31 m of height, and 4 cm of bark thickness), *Pouteria erythrochrysa* T.D.Penn (36.5 cm DBH, 29.3 m height, and 2 cm bark thickness) and *Eschweilera bracteosa* (Poepp. ex O.Berg) Miers (29.7 cm of DBH, 27 m of height, and 6 cm bark thickness) were selected for the study on the plateau (S 02° 36' 32'', W 60° 12' 32.9''). Each tree was within 15 m of the K34 tower such that their canopy branches were accessible from the tower. Diurnal field experiments occurred between June to October 2017 during the regular dry season. The mean value of rainfall is ~2,500 mm $year^{-1}$ with the driest months of the year concentrated from July to September (Araújo 2002).

The dynamic E_s gas-exchange system consisted of ¼" O.D. Teflon tubing and a dual channel infrared gas analyzer (IRGA) configured in differential mode (Li-7000, Li-Cor Inc., Lincoln, Nebraska, USA) to determine the difference (Δ) in [CO_2] between air entering (reference IRGA) and exiting (sample IRGA) an acrylic semi-cylinder chamber (324 ml in volume, 16.5 cm length and 10 cm width). The stem chamber was connected to the stem of the sample tree at 1.3 m height using a 5 cm thick foam to minimize air leaks and secured to the tree using two adjustable nylon slings. Ambient air at 0.5 m height above the ground was delivered to both the reference IRGA and the stem chamber by pumping (Laboport membrane pump, KNF Neuberger Inc., USA) from a 0.5 m^3 gas mixing box, to buffer fast changes in [CO_2], to the reference IRGA (100 ml min^{-1}) using a mass flow controller (FMA3704,

Omega Engineering, USA). In addition, ambient air was pumped (400 ml min^{-1}) into the chamber using a second mass flow controller (EW-32907-67, Cole Parmer, USA). The internal pump of the Li-7000 was used to draw sample air inside the chamber into the sample IRGA (50-100 ml min^{-1}). The excess flow entering the chamber escaped through the porous foam.

The system was calibrated each day before measurements begin with 0 ppm [CO_2] using a zero-air generator (Aadco 737, Aadco Inst., USA) with a downstream soda lime cartridge to scrub any remaining CO_2 from the ambient air. The calibration gas was placed into the reference IRGA and manually set to read 0 ppm. Following this, the output flow containing the 0 ppm calibration gas from the reference IRGA was delivered to the inlet of the sample IRGA. Following stabilization of the signals, the sample IRGA was manually set to 'match' the [CO_2] of the reference IRGA. To complete the two-point calibration procedure, the same process was then repeated using a 400 ppm [CO_2] calibration gas standard (Praxair Inc., USA). Validation of the system was provided by placing the chamber inside a plastic bag and verifying that the ΔCO_2 was less than 5 ppm. In addition, once installed on the sample tree, validation was also obtained when the ambient air flow entering the enclosure was increased resulting in a decrease in ΔCO_2, followed by a decrease in the ambient air flow entering the enclosure resulting in an increase in ΔCO_2. Experimental data included [CO_2] measurements from ambient air entering the dynamic stem enclosure and air exiting the enclosure were logged on a laptop computer at 1 Hz frequency continuously for up to 12 hours, followed by a 1-hour drying period of back flushing the tubing and Li-7000 system using dry air produced from the zero-air generator. Following the drying period, which was necessary to remove any condensed water, an additional 12 hours of data was logged. E_S (μmol CO_2 m^{-2} s^{-1}) was calculated based on **Eq 4.**

Equation 4: $$E_s = \frac{\Delta CO_2 F}{V t S}$$

Where ΔCO_2: difference between [CO_2] in the ambient air interring the chamber and inside the chamber (μL L^{-1}), F: ambient air flow rate entering the stem chamber (L min^{-1}), V: molar volume of an ideal gas

250 (24 L mol^{-1}), t: conversion factor of time from minutes to seconds (1 min/60 sec) and S: superficial stem
251 area enclosed by the chamber (0.016 m^2).

252 Sap velocity measurements were made every 15 minutes using a heat ratio sap flow sensor
253 (SFM1, ICT international) installed at 2.1 m (*P. anomala*), 2.0 m (*P. erythrochrysa*), and 1.7 m (*E.*
254 *bracteosa*) of height above the ground. The SFM1 sensors have three needles inserted parallel to the
255 stem and include a heating needle that emits a rapid pulse of 20 Joules of thermal energy and two
256 needles that determine sap temperature upstream and downstream of the heating needle at 0.75 cm and
257 2.25 cm of depth inside the xylem for 5 min 32 s following the heat pulse (Green et al. 2003;
258 Christianson et al. 2017). Sap velocity (cm hr^{-1}) was calculated using the Sap Flow Tool software
259 version 1.4.1 (Phyto-IT) from the raw sap temperature ratio data downloaded from the SFM1 sensors in
260 the field programmed to collect data every 15 min.

261 Tree crown temperature measurements were made with three infrared radiometer sensors (SI-
262 131, Apogee) installed on the K-34 tower and aimed at each tree crown (one IR sensor per tree) with
263 five-minute averages recorded on a data logger (CR-3000 Campbell Scientific). The IR sensors were
264 positioned at 28.8 m height and 4.25 m distance from the *P. anomala* crown, 25.3 m height and 6.55 m
265 from the *P. erythrochrysa* crown and 28.6 m height and 4.4 m from the *E. bracteosa* crown. To validate
266 the IR measurements of crown temperature, Teflon insulated thermocouples (type T, Omega
267 Engineering) were attached to the lower leaf surface of eight leaves in the crown of the *P. anomala*
268 individual during the two diurnal experiments. The thermocouple sensors were positioned on leaves in a
269 branch approximately 1 m from the flux tower structure at the same height as the IR sensor and
270 connected to a temperature recorder (OM-CP_OCTTEMP-A, Omega Engineering) that registered
271 average leaf temperatures every 15 seconds. In addition, Atmospheric vapor pressure deficit (VPD) was
272 calculated based on K-34 flux tower data collection of air temperature and relative humidity using a
273 thermohydrometer (HC2S3, Campbell Scientific) measured at 28 m during the period of this study
274 (Ewers and Oren, 2000). Air temperature and relative humidity was provided by the Large-Scale

275 Biosphere-Atmosphere (LBA) program at the National Institute for Amazon Research (INPA).

276

277 **3. Results**

278 *3.1 Stem growth and CO_2 efflux in the BIONTE experiment*

279 A total of 80 trees were studied across a broad range of growth rates and tree base diameters in
280 plots exhibiting variable rates of net biomass accumulation following a logging disturbance. The
281 supplementary data file (Tree_Diameter.xlsx) summarizes the collected biophysical properties of the 80
282 tree individuals including BIONTE treatment plot (T0-T3), tree ID, wood density (g ml^{-1}), and monthly
283 diameter DBH values (cm). While the individuals were not identified at the species level, the common
284 name in Brazilian Portuguese was recorded.

285 Following the selective logging, all BIONTE plots, including the control plots, experienced a
286 net increase in biomass over time (**Fig. 2**). Previous studies reported that tree growth rates and biomass
287 accumulation in the BIONTE control plots were greater than other control plots in nearby forests
288 (Chambers et al. 2001), indicating a lack of biomass steady-state in the BIONTE control plots. This
289 allowed for an analysis of the influence of growth on carbon allocation to stem respiration among the
290 high diversity of tree species in the BIONTE plots. For each individual in 2002, monthly average stem
291 diameter increment rates were determined (μm day^{-1}) with values reaching up to 60 μm day^{-1} for several
292 fast-growing individuals. A clear annual pattern in monthly average stem diameter increment rates was
293 observed with increased rates during the wet season (positive growth rates), and less positive and even
294 negative diameter increments for some individuals during the hot dry season (e.g. July-Sept) (**Fig. 3**).

295 Using the measured wood density of each stem, the average annual stem growth rate was then
296 calculated for each individual in the same units of stem CO_2 efflux according to **Eq. 2**. By plotting the
297 average annual stem CO_2 efflux (E_S, μmol CO_2 m^{-2} s^{-1}) against the average annual stem growth rate
298 expressed as a CO_2 flux (μmol CO_2 m^{-2} s^{-1}), several key results can be noted (**Fig. 4**). E_S values varied
299 by a factor of 10 from as low as 0.17 to as high as 1.7 μmol CO_2 m^{-2} s^{-1}. Likewise, stem growth rates

ranged from near zero to over 40 μm day^{-1}, or 5.0 μmol CO_2 m^{-2} s^{-1} when expressed as CO_2 flux. Despite the high variability in the data, a weak correlation between E_s and growth (R^2 of 0.3) was observed with E_S values tending to increase as a function of stem growth rates. Under zero growth, maintenance respiration (R_M) of BIONTE trees is estimated from the y-intercept of **Fig. 4** as 0.41 ± 0.04 μmol m^{-2} s^{-1} with the slope of the linear fit (0.15 ± 0.03 μmol m^{-2} s^{-1}) representing the respiratory carbon loss equivalent to 15 ± 3% of stem carbon accrual.

When the average annual carbon use efficiency (CUE_W) of wood was calculated for each individual, CUE_W was found to increase markedly with the average annual stem growth rate, reaching maximum values of 77-87% for a fast-growing tree (**Fig. 5**). CUE_W estimated using the observed average daytime E_S fluxes, were higher by 0.9-17% than CUE_W estimated from nighttime E_S fluxes, which were assumed to be 2-times higher during the night than during the day based on results from the diurnal E_S studies described in section 3.2 below.

3.2 Continuous observations of crown temperature, sap velocity, and E_s during the night and day for three trees near the K-34 tower

Each of the three individual trees studied near the K34 tower for real-time observations of stem CO_2 efflux were coupled together with continuous observations of sap velocity, crown temperature, and vapor pressure deficit (VPD). For each tree studied, crown temperature, VPD, and sap velocity generally tracked each other throughout both the day and night, but showed an apparent inverse relation with E_S (**Fig. 6**). During the day, a reduction of E_S by 14-50% relative to the fluxes at night were associated with high transpiration rates when crown temperatures exceeded 24-28.5°C (**Fig. 7**). For example, for the *P. anomala* individual during the day-time, the observed crown temperature range was about seven degrees (27-34°C), and the E_S range between 0.54-0.75 μmol m^{-2} s^{-1}, with the sap velocity between 7.0-8.6 cm hr^{-1}. Between 10:30-11:15, an increase in crown temperature occurred together with elevated sap velocities and this was associated with E_S suppression. In contrast, between 11:15-12:15,

the buildup of mid-day clouds reduced crown temperatures and VPD together with sap velocities while E_S increased to maximum values. Nonetheless, throughout the day there was a general trend of increasing crown temperature with VPD and sap velocity in the afternoon (12:45-14:00) and an E_S suppression. On the intervals between 10:30-10:35, 11:30-11:35 and 13:15-13:20, transient variations were observed in crown temperature and VPD with corresponding responses in E_S. For the *P. erythrochrysa* individual, the same general day-time pattern could be observed, with the maximum value of crown temperature occurring at the same time as minimum value of E_S (12:30). For the *E. bracteosa* individual, day-time VPD tracked crown temperature and sap velocity with E_S generally showing the opposite behavior. For example, between 12:30-13:30 when crown temperature and VPD decreased due to the buildup of mid-day clouds, an increase in E_S was observed. The apparent inverse relationship between crown temperature and E_S that was observed throughout the day for the three individual trees was also observed when daytime data was compared to data during the night. Relative to the day, the crown temperature and VPD reached a minimum at night, whereas the E_S reached a maximum (**Fig. 6b,d,f**).

When E_S was plotted against crown temperature and sap velocity, for the three individual trees studied near the K34 tower, a negative linear relationship was observed. With increases in crown temperature, VPD, and sap velocity, E_S tended to decrease (**Fig. 7a,c,e**). Good statistical fits between E_S and crown temperature were found using the polynomial $E_s = \beta_0 + \beta_1(\text{Crown Temperature}) + \beta_1(\text{Crown Temperature})^2$, with R^2 coefficients of 0.66, 0.15, and 0.65 respectively for *P. anomala*, *P. erythrochrysa*, and *E. bracteosa*. Similarly, by plotting E_S against sap velocity, good fits between E_S and sap velocity was achieved using the polynomial $E_s = \beta_0 + \beta_1(\text{sap velocity}) + \beta_1(\text{sap velocity})^2$. This analyses resulted in R^2 values of 0.48, 0.13, and 0.23, respectively, for *P. anomala*, *P. erythrochrysa*, and *E. bracteosa* (**Fig. 7b,d,f**). From this analysis, it was observed that above a threshold range of crown temperature (*P. anomala*: 24-25°C, *P. erythrochrysa*: 27.5-28.5°C, and *E. bracteosa*: 25.5-26.5°C) a suppression in E_S occurred and was associated with high sap velocities (> 2-7 cm hr^{-1}).

4. Discussion

Toward the goal of developing a more mechanistic understanding of the biological and environmental factors that influence autotrophic respiration in the tropics, in this study, we evaluated the hypothesis that variations in stem CO_2 efflux (E_S) are driven by changes in growth rates across both diurnal and annual time swhile the cales. This hypothesis was evaluated in a highly diverse 'terra-firme' tropical forest ecosystem in the central Amazon, by determining relationships between average annual stem growth (wood production, P_w) and stem CO_2 efflux (E_S) across 80 individuals. We also sought to evaluate the hypothesis across diurnal time scales by characterizing real-time diurnal patterns in E_S in connection with observations of sap velocity and estimates of leaf to atmosphere vapor pressure deficits (VPD), the 'driver' of plant transpiration. Early work showed a regular pattern in wood formation of many tropical tree species related to a distinct rainfall periodicity (Worbes 1995). During the dry season, changes in water availability together with increased atmospheric demand for water vapor (VPD) can drive higher transpiration rates leading to reductions in plant water content, stem diameter, and new wood production. In contrast, during the wet season when soil moisture is high, tree diameters can increase as a result of both refilling of plant water reservoirs together with new wood production (Dünisch et al. 2003; Schöngart et al. 2017). In order to minimize the influence of these hydraulic effects on growth rate estimates, we determined the average annual stem diameter increment and E_S fluxes for each individual.

Mean annual daytime E_S fluxes (0.55 ± 0.33 μmol m^{-2} s^{-1}), determined here for trees in the BIONTE plot during 2002, compare well with mean annual E_S fluxes (0.6 μmol m^{-2} s^{-1}) previously reported for Manaus and the Tapajos National Forest (Chambers et al. 2004; Trumbore 2006). However, to our knowledge, night time E_S fluxes have not yet been reported in the Amazon basin. In general, published measurements of E_S in the Amazon Basin have reported highly variable daytime observations from canopy trees (Nepstad 2002; Chambers et al. 2004; Malhi et al. 2009; Rowland et al.

375 2018). For example, Chambers et al., 2004, values ranged over two orders of magnitude (0.027 to 3.64
376 μmol m^{-2} s^{-1}) with the large variation largely unexplained. In this study across the 80 individuals,
377 daytime E_S values also varied substantially by a factor of 10 from as low as 0.17 to as high as 1.7 μmol
378 CO_2 m^{-2} s^{-1}. By observing a statistically significant positive linear relationship between annual average
379 stem growth rates and E_S, we show that some of this variability in E_S can be attributed to tree growth
380 rates (which ranged from near zero with little net annual growth to over 40 μm day^{-1}). Thus, the fastest
381 growing stems tended to have the highest rates of E_S while individuals showing little to no growth
382 tended to have lower rates of E_S. In addition, the slope of the linear relationship was determined to be
383 0.15 ± 0.03, suggesting that between 12 and 18% of total carbon allocated to stems is respired and
384 released to the atmosphere as CO_2. These findings are consistent with previous studies in the Tapajos
385 National Forest in the Amazon (Nepstad 2002) and a Costa Rican forest (Ryan et al. 1994) where E_S
386 was positively correlated with tree growth rates.

387 Moreover, when stem growth rates were expressed in the same units as E_S, CUE_W was found to
388 increase with stem growth rates, with maximum CUE_W for a fast-growing tree reaching values between
389 77-87%. CUE_W provides a measure of what fraction of total carbon assimilation becomes incorporated
390 into new woody tissues. Previous studies in the ZF2 forest preserve outside of Manaus, Brazil estimated
391 average CUE_W of 43% (Chambers et al. 2004) while a second study estimated values ranging from 30-
392 56% for Manaus (46%), Tapajós (56%), and Caxiuanã (30%) (Malhi et al. 2009). Our results from the
393 BIONTE experiment near Manaus suggest that high CUE_W values (up to 77-87%) are associated with
394 high daytime E_S fluxes during fast tree growth. Therefore, trees with higher daytime E_S fluxes tend to be
395 faster growing and with higher CUE_W values.

396 Using real-time data from three canopy trees, we also show that E_S variability is inversely
397 linked to crown temperature/VPD and sap velocity on diurnal time scales. VPD tracked crown
398 temperature and sap velocity throughout both the day and night. This is consistent with a recent study
399 using a larger set of trees near the K34 tower (including the three that were studied here), which showed

400 that sap velocity, leaf temperature, and leaf to air-VPD were positively correlated during both the day
401 and night with no detectable delay between the variables (<15 min) (Gimenez et al. 2019). Despite large
402 height differences between E_S and sap velocity measurements at the base of the stem and crown
403 temperature and VPD observations at 25-29 m within the canopy, E_S was inversely related to these
404 variables at minute to diurnal time scales. A strong (15-50%) E_S suppression was observed during the
405 daytime relative to the night associated with elevated values of crown temperature/VPD and high
406 transpiration rates. These findings are consistent with a previous study at the same Amazon field site on
407 a single *Scleronema micranthum* (Ducke) Ducke individual that found higher E_S fluxes at night relative
408 to the day with E_S fluxes decreasing with the commencement of xylem sap velocity and elevating air
409 temperature in the early morning (N. Kunert, 2018). These patterns are alternate to what would be
410 expected simply due to changes in stem temperature that increase during the day, which stimulate
411 respiration due to its Q10 thermal dependence. Thus, the mechanism of daytime E_S suppression cannot
412 be explained by the impact of temperature on respiration.

413 Due to the use of sealed static stem enclosures which report only an averaged E_S flux over the
414 measurement period, previous studies of E_S fluxes from Neotropical rainforests reported little
415 information on potential diurnal patterns including studies in French Guiana (Stahl et al. 2011), the
416 central Amazon (Chambers et al. 2004), and the eastern Amazon (Rowland et al. 2018). However,
417 diurnal studies in subtropical China reported E_S fluxes increasing during the daytime following closely
418 the diurnal increases in temperature, enabling an estimate of E_S Q10 values (Yang et al. 2012).
419 Similarly, diurnal E_S studies from woody stems of eudicots and gymnosperms in Guam, Thailand, and
420 the Philippines showed diurnal E_s fluxes that were 36-40% greater than nighttime E_s (Marler et al.,
421 2020). Based on these and other field measurements, a previous statistical global model predicted that
422 E_S increases with temperature in the tropics (Yang et al. 2016). For example, on a global annual basis,
423 E_S was suggested to increase with temperature with annual E_S values in the Amazon Basin estimated
424 three-to-five times greater than E_S fluxes for temperate and Boreal forests.

425 Although additional research is needed to resolve why some studies have reported positive daytime
426 increases in E_S together with transpiration and temperature while others have observed a clear daytime
427 suppression in E_S, one possibility may be the variable influence of root/soil respiratory sources of CO_2.
428 E_S observations at height of 1.3 m, as performed here in the central Amazon, may be sufficiently high to
429 avoid a significant impact of soil/root derived CO_2 on observed stem Es fluxes. In contrast, the
430 southeast Asia study in Guam, Thailand, and the Philippines quantified diurnal stem Es fluxes at a much
431 lower stem height of 0.3-0.4 m, and did not observe daytime suppression relative to the night (Marler et
432 al., 2020). Stem diameters were a similar range in the southeast Asia study (29 to 92 cm) and central
433 Amazon (BIONTE: 10-52 cm, K34 tower: 30-37 cm) studies reported here. Thus, we assume stem Es
434 fluxes observations in the central Amazon are mainly influenced by respiratory processes in the local
435 sap wood at the height of measurement (1.3 m), rather than roots/soils. However, additional research is
436 needed to characterize the relative importance of autotrophic and heterotrophic sources of stem Es flux
437 as a function of height in tropical trees.
438 Nonetheless, the suppression of E_S associated with high daytime temperatures and transpiration,
439 as observed here in the central Amazon, are consistent with a similar finding reported at the same
440 Amazon field site on a single *Scleronema micranthum* (Ducke) Ducke individual (N. Kunert, 2018), as
441 well as numerous greenhouse and field studies outside the tropics. Although mitochondrial respiration is
442 known to increase with temperature (Atkin and Tjoelker 2003; Noctor et al. 2007), a growing number
443 of studies outside of the tropics have shown that daytime E_S can be suppressed during the day relative to
444 the night. For example, results from an experimental forest in Georgia showed both reduced
445 transpiration rates and enhanced E_S at night relative to the day, despite substantially higher temperatures
446 during the day compared to the night (Maier and Clinton 2006). Mechanistic studies suggested that
447 daytime suppression of E_S is strongly related to stem water potential decreases that inhibit growth and
448 its associated respiratory fluxes (Saveyn et al. 2007). Indeed, stem growth rates of several tree species

449 have been documented to be higher at night than the day (Nozue et al. 2007). Although early studies
450 reporting daytime E_S suppression mainly discussed a possible role of transport of CO_2 in the
451 transpiration stream, an alternative mechanism was proposed (Saveyn et al. 2007) based on the daily
452 dynamics of turgor pressure. The daytime decrease in stem water potential was hypothesized to be a
453 key determinant of E_S through its direct negative influences on the rates of growth and maintenance
454 processes in the living tissues of the stem.

455 Numerous other studies have shown a tendency of a suppression in E_S during periods of high
456 transpiration (Levy et al. 1999; Teskey and McGuire 2007; Bowman et al. 2008). These and other
457 studies suggested that a suppression of E_S during day-time periods of high sap flow may be a result of
458 numerous processes including enhanced CO_2 storage (Bowman et al. 2005; Teskey and McGuire 2007;
459 Robert O. Teskey, An Saveyn, Kathy Steppe, Mary Anne McGuire 2007; Teskey et al. 2008), increased
460 respiratory CO_2 transport via the transpiration stream (Katayama et al. 2014), a suppression of
461 mitochondrial respiration and growth by reduced daytime xylem water potential (Saveyn et al. 2007),
462 enhanced re-assimilation of respiratory CO_2 through both light-dependent photosynthetic green-tissue
463 assimilation (Wittmann et al. 2006), and light-independent bicarbonate fixation via phosphoenol
464 pyruvate carboxylase activity involved in the biosynthesis of dicarboxylic acids like malate that are
465 used as respiratory substrates (Berveiller and Damesin 2008). Thus, an E_S and growth suppression could
466 have major implications for stress coping mechanisms during high temperature and droughts such as
467 those experienced during ENSO events (Longo et al. 2018). As has been previously discussed based on
468 CO_2 re-assimilation studies (Bloemen et al. 2013a, b), an increased transport of respired CO_2 could
469 result in enhancing internal CO_2 re-assimilation within stems and leaves and consequently contribute to
470 protective mechanisms during climate extremes. Moreover, a downregulation of growth and respiratory
471 processes during climate warming and drought may act to increase survivability through conservation
472 of valuable respiratory substrates such as non-structural carbohydrates whose exhaustion could lead to
473 carbon starvation and mortality (McDowell and Sevanto 2010).

While the proposed mechanisms of daytime E_S suppression are not mutually exclusive, they are reportedly difficult to disentangle. However, more recent studies have attempted to discriminate between internal transport/re-assimilation versus attenuated respiratory activity due to lower turgor pressure. For example, when manipulative greenhouse studies were performed by defoliation and drought treatments, only turgor pressure was a robust predictor of daytime suppression of temperature-normalized E_S fluxes (Salomón et al. 2018). Regardless of the mechanisms of E_S suppression, we confirm that strong daytime stem E_S suppression can occur in Amazon trees during warm periods associated with high rates of transpiration. Despite similar findings outside of the tropics, we acknowledge however, that our findings are restricted to a limited number of trees with measurements capturing only one diurnal period. While verification of a daytime suppression of E_S associated with high transpiration rates among highly diverse canopy dominant trees in the Amazon and other tropical forests requires additional research, the observations are consistent with the emerging view that diurnal dynamics of stem water fluxes influence CO_2 transport, metabolism, and E_S as well as respiratory processes associated with stem growth.

5. Data and Materials Availability

All data presented in the manuscript, including raw (diameter and wood density) and derived (E_S, growth rates, and growth rates as CO_2 efflux) datasets from the 80 trees in the BIONTE central Amazon field site are available for public download and use from the NGEE Tropics data archive (NGT0168, Stem CO_2 Efflux and growth rates in a selectively logged experiment in the central Amazon 2001-2002, http://dx.doi.org/10.15486/ngt/1767825). In addition to the raw and derived data, important metadata is also available including sampling date and location, tree ID, genus, species, family, tree number, research site, data measurement variables and units. A second data set is also available which includes real time E_s from three canopy dominant trees together with canopy temperature and sap flow during the day and night (NGT0149, Stem CO_2 Efflux measurements from

Manaus, Brazil 2017, http://dx.doi.org/10.15486/ngt/1804760). Data users can view the public datasets and all related metadata through the NGEE Tropics data archive. Once users register with a FluxNet ID, which only requires an email to sign up, the datasets are free to download and use in future experimental and modeling studies focused on understanding the roles of autotrophic respiration and growth in ecosystem carbon storage and cycling.

6. Acknowledgements

This material is based upon work supported as part of the Next Generation Ecosystem Experiments-Tropics (NGEE-Tropics) funded by the U.S. Department of Energy, Office of Science, Office of Biological and Environmental Research through contract No. DE-AC02-05CH11231 to LBNL, as part of DOE's Terrestrial Ecosystem Science Program. This work was also supported in part by the US Department of Energy, Office of Science, Office of Workforce Development for Teachers and Scientists (WDTS) under the Science Undergraduate Laboratory Internship (SULI) Program and the Brazilian fund: "Coordenação de Aperfeiçoamento de Pessoal de Nível Superior" (CAPES). We would like to kindly acknowledge the field logistics support by the forest management department at the National Institute for Amazon Research (INPA) in Manaus, Brazil.

7. Author Contributions

K.J., L.T., L.O., and B.G. collected all field data with J. C., and N. H. supervising the projects. E.R. facilitated archiving of the datasets on the NGEE-Tropics archive. All authors discussed the results and contributed to the development of the final manuscript.

8. References

522 Amthor JS (2000a) Direct effect of elevated CO_2 on nocturnal in situ leaf respiration in nine temperate
523 deciduous tree species is small. Tree Physiol 20:139–144.
524 https://doi.org/10.1093/treephys/20.2.139

525 Amthor J (2000b) The mccree–de wit–penning de vries–thornley respiration paradigms: 30 years later.
526 Ann Bot 86:1–20. https://doi.org/10.1006/anbo.2000.1175

527 Araújo AC (2002) Comparative measurements of carbon dioxide fluxes from two nearby towers in a
528 central Amazonian rainforest: The Manaus LBA site. J Geophys Res 107:8090.
529 https://doi.org/10.1029/2001JD000676

530 Atkin OK, Macherel D (2009) The crucial role of plant mitochondria in orchestrating drought tolerance.
531 Ann Bot 103:581–597. https://doi.org/10.1093/aob/mcn094

532 Atkin OK, Tjoelker MG (2003) Thermal acclimation and the dynamic response of plant respiration to
533 temperature. Trends Plant Sci 8:343–351. https://doi.org/10.1016/S1360-1385(03)00136-5

534 Aubrey DP, Teskey RO (2009) Root-derived CO_2 efflux via xylem stream rivals soil CO_2 efflux. New
535 Phytol 184:35–40. https://doi.org/10.1111/j.1469-8137.2009.02971.x

536 Berveiller D, Damesin C (2008) Carbon assimilation by tree stems: potential involvement of
537 phosphoenolpyruvate carboxylase. Trees 22:149–157. https://doi.org/10.1007/s00468-007-0193-4

538 Bloemen J, McGuire MA, Aubrey DP, et al (2013a) Transport of root-respired CO_2 via the
539 transpiration stream affects aboveground carbon assimilation and CO_2 efflux in trees. New Phytol
540 197:555–565. https://doi.org/10.1111/j.1469-8137.2012.04366.x

541 Bloemen J, McGuire MA, Aubrey DP, et al (2013b) Internal recycling of respired CO_2 may be
542 important for plant functioning under changing climate regimes. Plant Signal Behav 8:e27530.
543 https://doi.org/10.4161/psb.27530

544 Bowman WP, Barbour MM, Turnbull MH, et al (2005) Sap flow rates and sapwood density are critical
545 factors in within- and between-tree variation in CO_2 efflux from stems of mature Dacrydium
546 cupressinum trees. New Phytol 167:815–828. https://doi.org/10.1111/j.1469-8137.2005.01478.x

547 Bowman WP, Turnbull MH, Tissue DT, et al (2008) Sapwood temperature gradients between lower
548 stems and the crown do not influence estimates of stand-level stem CO_2 efflux. Tree Physiol
549 28:1553–1559. https://doi.org/10.1093/treephys/28.10.1553

550 Chambers JQ, Santos J dos, Ribeiro RJ, Higuchi N (2001) Tree damage, allometric relationships, and
551 above-ground net primary production in central Amazon forest. Forest Ecology and Management
552 152:73–84. https://doi.org/10.1016/S0378-1127(00)00591-0

553 Chambers JQ, Silver WL (2004) Some aspects of ecophysiological and biogeochemical responses of
554 tropical forests to atmospheric change. Philos Trans R Soc Lond B Biol Sci 359:463–476.
555 https://doi.org/10.1098/rstb.2003.1424

556 Chambers JQ, Tribuzy ES, Toledo LC, et al (2004) Respiration from a tropical forest ecosystem:
557 partitioning of sources and low carbon use efficiency. Ecol Appl 14:72–88.
558 https://doi.org/10.1890/01-6012

559 Christianson DS, Varadharajan C, Christoffersen B, et al (2017) A metadata reporting framework
560 (FRAMES) for synthesis of ecohydrological observations. Ecol Inform.
561 https://doi.org/10.1016/j.ecoinf.2017.06.002

562 Clark DA (2004) Sources or sinks? The responses of tropical forests to current and future climate and
563 atmospheric composition. Philos Trans R Soc Lond B Biol Sci 359:477–491.
564 https://doi.org/10.1098/rstb.2003.1426

565 da Silva RP, dos Santos J, Tribuzy ES, et al (2002) Diameter increment and growth patterns for
566 individual tree growing in Central Amazon, Brazil. Forest Ecology and Management 166:295–301.
567 https://doi.org/10.1016/S0378-1127(01)00678-8

568 Dünisch O, Montóia VR, Bauch J (2003) Dendroecological investigations on Swietenia macrophylla
569 King and Cedrela odorata L. (Meliaceae) in the central Amazon. Trees 17:244–250. https://doi.org/
570 10.1007/s00468-002-0230-2

571 Feeley KJ, Joseph Wright S, Nur Supardi MN, et al (2007) Decelerating growth in tropical forest trees.
572 Ecol Lett 10:461–469. https://doi.org/10.1111/j.1461-0248.2007.01033.x

573 Gaui TD, Costa FRC, Coelho de Souza F, et al (2019) Long-term effect of selective logging on floristic
574 composition: A 25 year experiment in the Brazilian Amazon. Forest Ecology and Management
575 440:258–266. https://doi.org/10.1016/j.foreco.2019.02.033

576 Gimenez BO, Jardine KJ, Higuchi N, et al (2019) Species-Specific Shifts in Diurnal Sap Velocity
577 Dynamics and Hysteretic Behavior of Ecophysiological Variables During the 2015-2016 El Niño
578 Event in the Amazon Forest. Front Plant Sci 10:830. https://doi.org/10.3389/fpls.2019.00830

579 Green S, Clothier B, Jardine B (2003) Theory and practical application of heat pulse to measure sap
580 flow. Agron J 95:1371–1379. https://doi.org/10.2134/agronj2003.1371

581 Higuchi N, Ferraz JBS, Antony L, Luizão FJ (1997) Biomassa e nutrientes florestais. Projeto BIONTE.
582 MCT-INPA, DFID.

583 Katayama A, Kume T, Komatsu H, et al (2014) Vertical variations in wood CO_2 efflux for live
584 emergent trees in a Bornean tropical rainforest. Tree Physiol 34:503–512.
585 https://doi.org/10.1093/treephys/tpu041

586 Körner C (2009) Responses of Humid Tropical Trees to Rising CO_2. Annu Rev Ecol Evol Syst 40:61–
587 79. https://doi.org/10.1146/annurev.ecolsys.110308.120217

588 Kunert, N (2018) A case study on the vertical and diurnal variation of stem CO_2 effluxes in an
589 Amazonian forest tree. Trees 32:913–917. https://doi.org/10.1007/s00468-018-1680-5Le Quéré C,
590 Andrew RM, Friedlingstein P, et al (2018) Global carbon budget 2018. Earth Syst Sci Data
591 10:2141–2194. https://doi.org/10.5194/essd-10-2141-2018

592 Levy PE, Meir P, Allen SJ, Jarvis PG (1999) The effect of aqueous transport of CO_2 in xylem
593 sap on gas exchange in woody plants. Tree Physiol 19:53–58.
594 https://doi.org/10.1093/treephys/19.1.53

595 Lloyd J, Farquhar GD (2008) Effects of rising temperatures and [CO_2] on the physiology of tropical
596 forest trees. Philos Trans R Soc Lond B Biol Sci 363:1811–1817.
597 https://doi.org/10.1098/rstb.2007.0032

598 Longo M, Knox RG, Levine NM, et al (2018) Ecosystem heterogeneity and diversity mitigate Amazon
599 forest resilience to frequent extreme droughts. New Phytol 219:914–931.
600 https://doi.org/10.1111/nph.15185

601 Luyssaert S, Inglima I, Jung M, et al (2007) CO_2 balance of boreal, temperate, and tropical forests
602 derived from a global database. Glob Chang Biol 13:2509–2537. https://doi.org/10.1111/j.1365-
603 2486.2007.01439.x

604 Maier CA, Clinton BD (2006) Relationship between stem CO_2 efflux, stem sap velocity and xylem CO_2
605 concentration in young loblolly pine trees. Plant Cell Environ 29:1471–1483.
606 https://doi.org/10.1111/j.1365-3040.2006.01511.x

607 Malhi Y, Aragão LEOC, Metcalfe DB, et al (2009) Comprehensive assessment of carbon productivity,
608 allocation and storage in three Amazonian forests. Glob Chang Biol 15:1255–1274. https://doi.org/
609 10.1111/j.1365-2486.2008.01780.x

610 Marler, TE, Lindström AJ (2020). Diel patterns of stem CO_2 efflux vary among cycads, arborescent
611 monocots, and woody eudicots and gymnosperms. Plant Signaling & Behavior 15: e1732661.
612 https://doi: 10.1080/15592324.2020.1732661.

613 McDowell NG, Marshall JD, Qi J, Mattson K (1999) Direct inhibition of maintenance respiration in
614 western hemlock roots exposed to ambient soil carbon dioxide concentrations. Tree Physiol
615 19:599–605. https://doi.org/10.1093/treephys/19.9.599

616 McDowell NG, Sevanto S (2010) The mechanisms of carbon starvation: how, when, or does it even
617 occur at all? New Phytol 186:264–266. https://doi.org/10.1111/j.1469-8137.2010.03232.x

618 McGuire MA, Teskey RO (2004) Estimating stem respiration in trees by a mass balance approach that
619 accounts for internal and external fluxes of CO_2. Tree Physiol 24:571–578. https://doi.org/10.1093/
620 treephys/24.5.571

621 Nepstad DC (2002) The effects of partial throughfall exclusion on canopy processes, aboveground
622 production, and biogeochemistry of an Amazon forest. J Geophys Res 107:.
623 https://doi.org/10.1029/2001JD000360

624 Nobre CA, Sampaio G, Borma LS, et al (2016) Land-use and climate change risks in the Amazon and
625 the need of a novel sustainable development paradigm. Proc Natl Acad Sci USA 113:10759–
626 10768. https://doi.org/10.1073/pnas.1605516113

627 Noctor G, De Paepe R, Foyer CH (2007) Mitochondrial redox biology and homeostasis in plants.
628 Trends Plant Sci 12:125–134. https://doi.org/10.1016/j.tplants.2007.01.005

629 Nozue K, Covington MF, Duek PD, et al (2007) Rhythmic growth explained by coincidence between
630 internal and external cues. Nature 448:358–361. https://doi.org/10.1038/nature05946

631 O'Leary BM, Asao S, Millar AH, Atkin OK (2019) Core principles which explain variation in
632 respiration across biological scales. New Phytol 222:670–686. https://doi.org/10.1111/nph.15576

633 Otani T, Lima AJ, Suwa R, et al (2018) Recovery of above-ground tree biomass after moderate
634 selective logging in a central Amazonian forest. iForest 11:352–359.
635 https://doi.org/10.3832/ifor2534-011

636 Robert O. Teskey, An Saveyn, Kathy Steppe, Mary Anne McGuire (2007) Origin, fate and significance
637 of CO_2 in tree stems. http://Robert O. Teskey, An Saveyn, Kathy Steppe, Mary Anne McGuire.
638 Accessed 23 Mar 2021

639 Rowland L, da Costa ACL, Oliveira AAR, et al (2018) Drought stress and tree size determine stem
640 CO2 efflux in a tropical forest. New Phytol 218:1393–1405. https://doi.org/10.1111/nph.15024

641 Rowland L, Hill TC, Stahl C, et al (2014) Evidence for strong seasonality in the carbon storage and
642 carbon use efficiency of an Amazonian forest. Glob Chang Biol 20:979–991.
643 https://doi.org/10.1111/gcb.12375

644 Ryan MG, Hubbard RM, Clark DA, Sanford RL (1994) Woody-tissue respiration for Simarouba amara
645 and Minquartia guianensis, two tropical wet forest trees with different growth habits. Oecologia
646 100:213–220. https://doi.org/10.1007/BF00316947

647 Salomón RL, De Schepper V, Valbuena-Carabaña M, et al (2018) Daytime depression in temperature-
648 normalised stem CO_2 efflux in young poplar trees is dominated by low turgor pressure rather than
649 by internal transport of respired CO_2. New Phytol 217:586–598. https://doi.org/10.1111/nph.14831

650 Saveyn A, Steppe K, Lemeur R (2007) Daytime depression in tree stem CO_2 efflux rates: is it caused by
651 low stem turgor pressure? Ann Bot 99:477–485. https://doi.org/10.1093/aob/mcl268

652 Schöngart J, Bräuning A, Barbosa ACMC, et al (2017) Dendroecological studies in the neotropics:
653 history, status and future challenges. In: Amoroso MM, Daniels LD, Baker PJ, Camarero JJ (eds)
654 Dendroecology: Tree-Ring Analyses Applied to Ecological Studies. Springer International
655 Publishing, Cham, pp 35–73

Stahl C, Burban B, Goret J-Y, Bonal D (2011) Seasonal variations in stem CO_2 efflux in the Neotropical rainforest of French Guiana. Ann For Sci 68:771–782. https://doi.org/10.1007/s13595-011-0074-2

Teskey RO, McGuire MA (2007) Measurement of stem respiration of sycamore (Platanus occidentalis L.) trees involves internal and external fluxes of CO_2 and possible transport of CO_2 from roots. Plant Cell Environ 30:570–579. https://doi.org/10.1111/j.1365-3040.2007.01649.x

Teskey RO, Saveyn A, Steppe K, McGuire MA (2008) Origin, fate and significance of CO2 in tree stems. New Phytol 177:17–32. https://doi.org/10.1111/j.1469-8137.2007.02286.x

Trumbore S (2006) Carbon respired by terrestrial ecosystems - recent progress and challenges. Global Change Biol 12:141–153. https://doi.org/10.1111/j.1365-2486.2006.01067.x

Valentini R, Matteucci G, Dolman AJ, et al (2000) Respiration as the main determinant of carbon balance in European forests. Nature 404:861–865. https://doi.org/10.1038/35009084

Vanlerberghe GC, Dahal K, Alber NA, Chadee A (2020) Photosynthesis, respiration and growth: A carbon and energy balancing act for alternative oxidase. Mitochondrion 52:197–211. https://doi.org/10.1016/j.mito.2020.04.001

Wittmann C, Pfanz H, Loreto F, et al (2006) Stem CO_2 release under illumination: corticular photosynthesis, photorespiration or inhibition of mitochondrial respiration? Plant Cell Environ 29:1149–1158. https://doi.org/10.1111/j.1365-3040.2006.01495.x

Worbes M (1995) How to measure growth dynamics in tropical trees a review. IAWA J 16:337–351. https://doi.org/10.1163/22941932-90001424

Yang J, He Y, Aubrey DP, et al (2016) Global patterns and predictors of stem CO_2 efflux in forest ecosystems. Glob Chang Biol 22:1433–1444. https://doi.org/10.1111/gcb.13188

Yang Q, Xu M, Chi Y, et al (2012) Temporal and spatial variations of stem CO_2 efflux of three species in subtropical China. Journal of Plant Ecology 5:229–237. https://doi.org/10.1093/jpe/rtr023

679
680

9. Figures

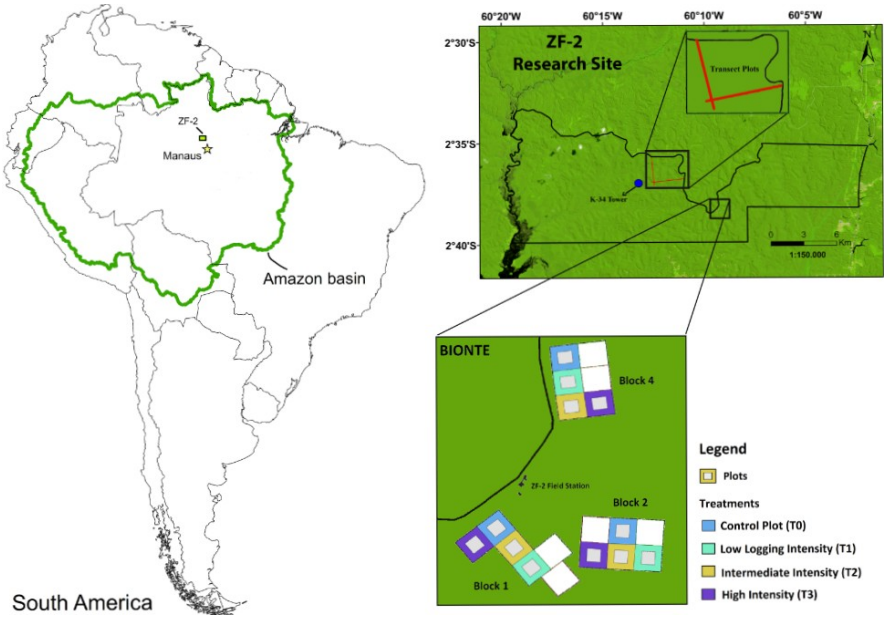

Figure 1: Schematic diagram of the BIONTE logging experiment showing the three experimental blocks, the layout of each 4-ha sub-blocks, and the location of the forest sample plot within each sub-block. Also shown is the location of the K34 tower where diurnal E_S flux studies were conducted together with observations of transpiration and its environmental drivers.

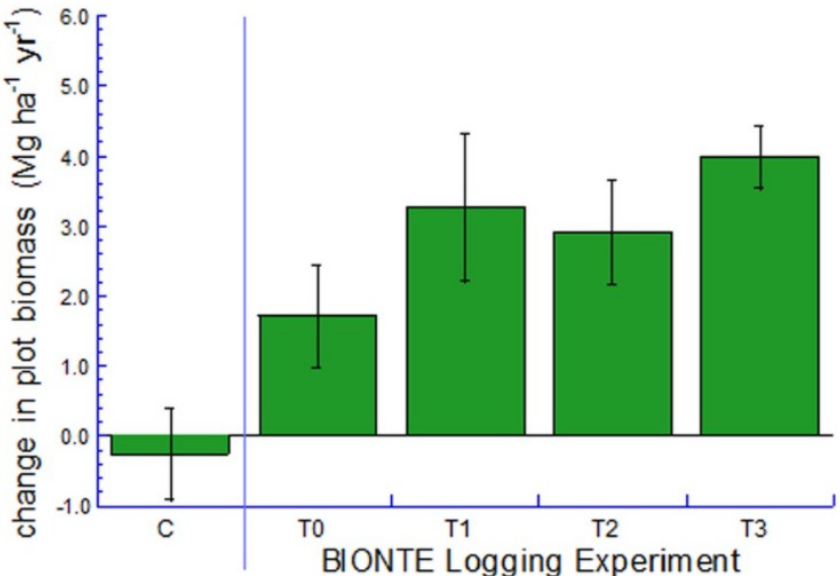

Figure 2: Net change in total above-ground tree biomass for the Transect control plots (C) and the BIONTE logging treatment plots (T0-T3). All BIONTE plots including the BIONTE control plots (T0)

experienced long-term biomass accumulation, in contrast to the Transect control plots that exhibited biomass steady-state.

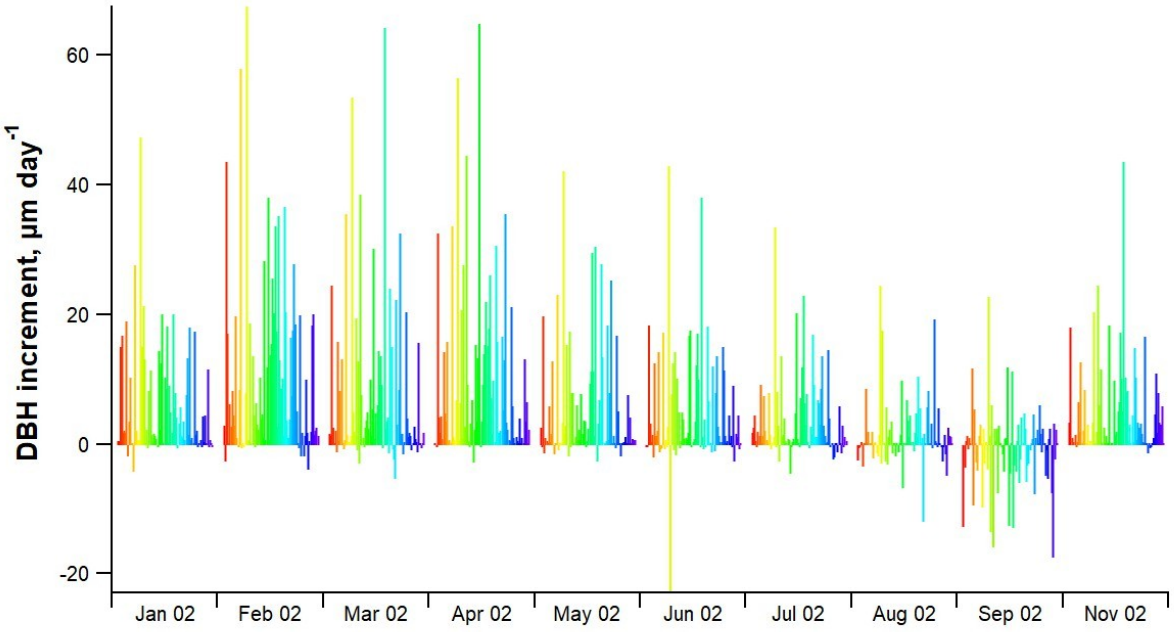

Figure 3: Monthly average stem diameter increments during 2002 for individual trees (n = 80 trees) in the BIONTE plots.

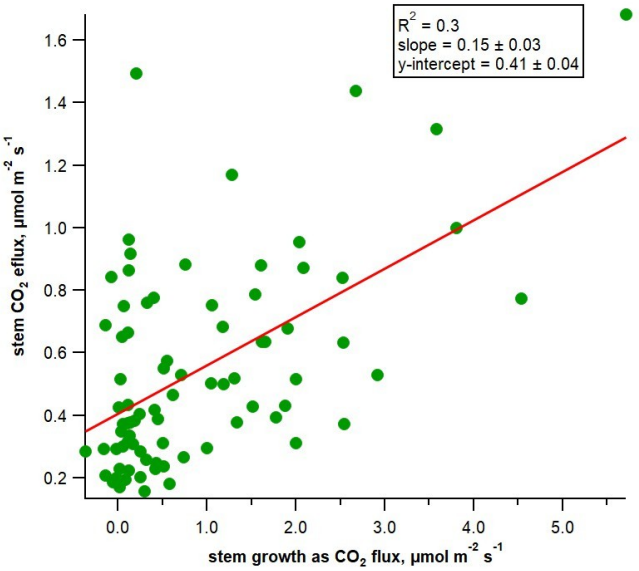

Figure 4. Average E_S rates plotted versus stem growth rates expressed as a CO_2 flux. Each point

700 represents average annual growth and respiration rate (in μmol m^{-2} s^{-1}) for individual trees (n = 80
701 trees) in the BIONTE plots. Note the trend of increased E_S fluxes as a function of stem growth rates.
702 Note that slope of the linear fit (0.15 ± 0.03 μmol m^{-2} s^{-1}) representing the respiratory carbon loss
703 equivalent to 15 ± 3% of stem carbon accrual. Maintenance respiration (R_M) is estimated as the y-
704 intercept = 0.41 ± 0.04 mol m^{-2} s^{-1}.
705

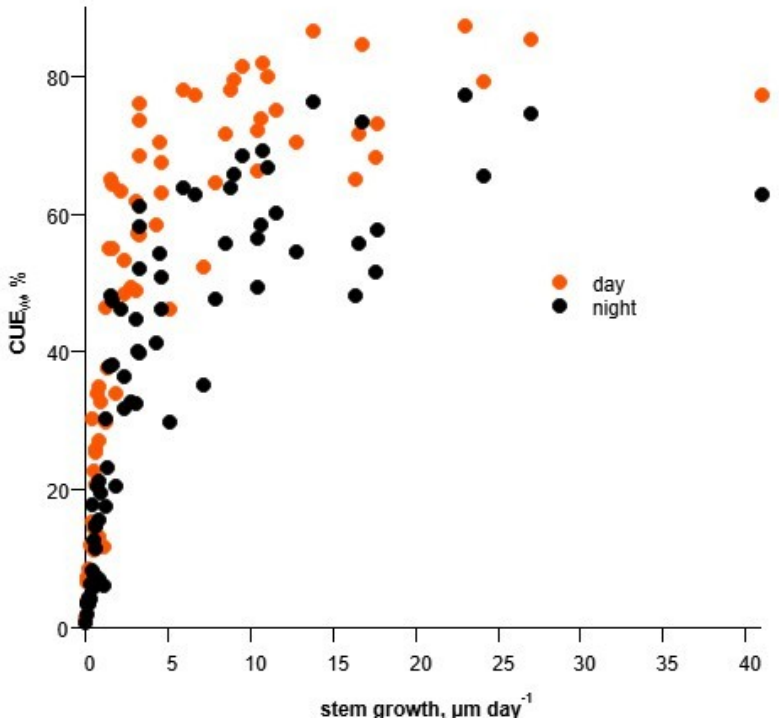

706
707 **Figure 5**: Change in estimated CUE_W from Es data plotted as a function of tree growth rate across the
708 80 tree individuals studied in the BIONTE plots. Note, CUE_W was estimated using the observed
709 average daytime E_S fluxes (orange points). Nighttime CUE_W was estimated by assuming nighttime E_S
710 fluxes are 2X higher than during the daytime (black points).

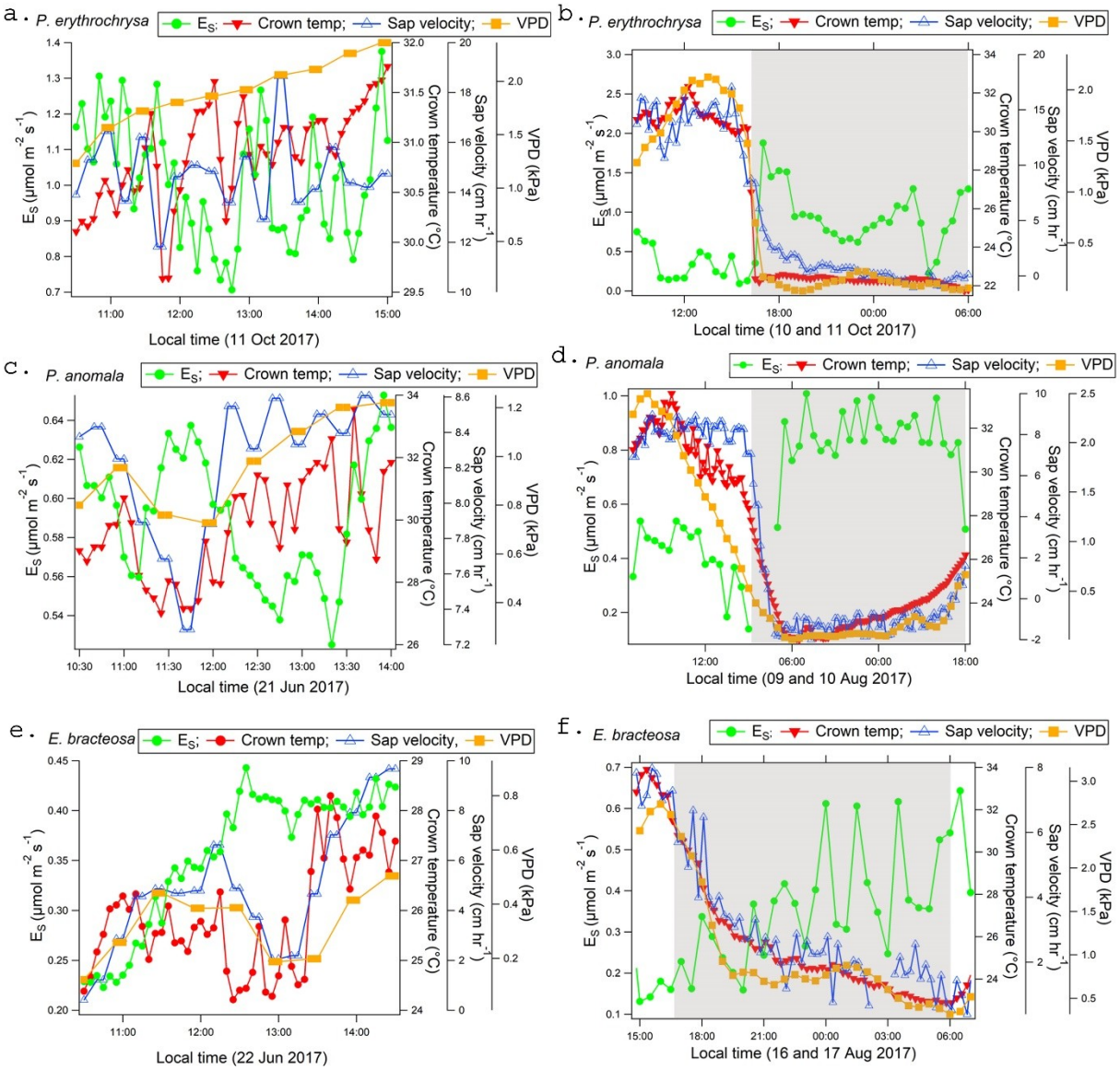

Figure 6: Example of high temporal dynamics (5 min) of basal E_S (µmol m^{-2} s^{-1}, 1.3 m) and Sap velocity (cm hr^{-1}, 1.5 m) together with crown temperature (°C, 28.8, 25.3 and 28.6 m) measured with an IR radiometer during a 4-hour period at the hottest hour of the day for: **a.** *P. anomala* (21 Jun 2017), **c.** *P. erythrochrysa* (11 Oct 2017) and **e.** *E. bracteosa* (22 Jun 2017). Also shown are diurnal patterns of E_S (30 min average), crown temperature and sap velocity (15 min averages) for three trees: **b.** *P. anomala*, **d.** *P. erythrochrysa* and **f.** *E. bracteosa*) showing higher E_S values during the night-time when crown temperature and sap velocity are low. Shaded areas in parts **b.**, **d.**, and **e.** represent nighttime data.

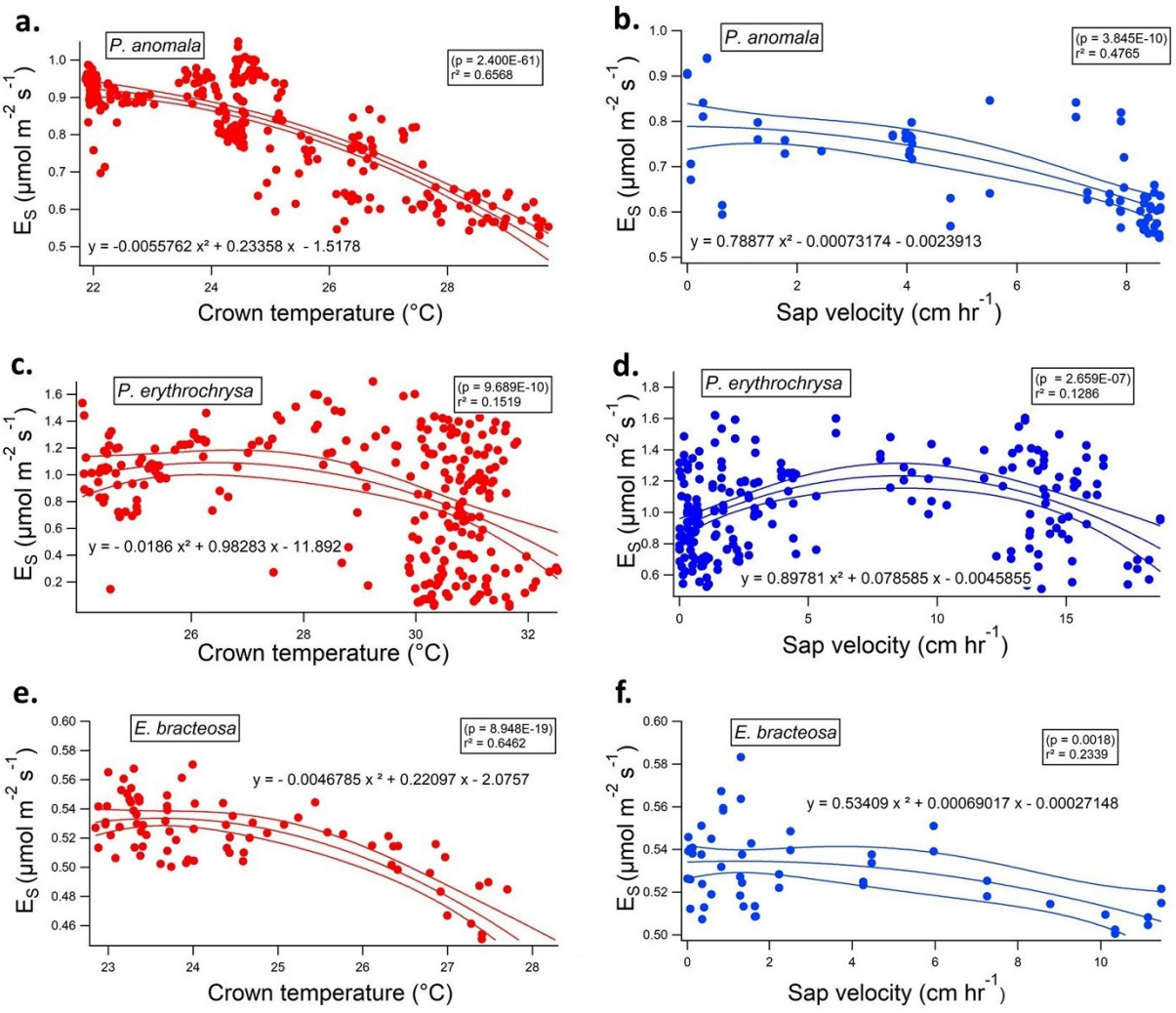

Figure 7. Scatter plots and nonlinear regression analyses of E_S versus crown temperature (hourly averages, red points) and E_s versus sap velocity (hourly averages, blue points) for three canopy dominant trees in the central Amazon: **a.** and **b.** *P. anomala* on 21 Jun 2017; **c.** and **d.** *P. erythrochrysa* on 11 Oct 2017; **e.** and **f.** *E. bracteosa* 22 Jun 2017). The central line represents the polynomial fit (see included equations) and the two other lines represents ± confidence interval. Regression statistics with 95% probability provided with p-value and R-Squared at the top-right corner of the plots.